A direct classical trajectory study of the acetone photodissociation on the triplet surface

ARTICLE *in* THE JOURNAL OF CHEMICAL PHYSICS · NOVEMBER 2003

Impact Factor: 2.95 · DOI: 10.1063/1.1622387

6 AUTHORS, INCLUDING:

Emilio Martinez-Nuñez
University of Santiago de Compostela
85 PUBLICATIONS **1,015** CITATIONS
SEE PROFILE

Antonio Fernández-Ramos
University of Santiago de Compostela
84 PUBLICATIONS **1,812** CITATIONS
SEE PROFILE

Natália D. S. Cordeiro
University of Porto
245 PUBLICATIONS **2,999** CITATIONS
SEE PROFILE

Saulo A Vázquez
University of Santiago de Compostela
89 PUBLICATIONS **1,041** CITATIONS
SEE PROFILE

A direct classical trajectory study of the acetone photodissociation on the triplet surface

E. Martínez-Núñez, A. Fernández-Ramos, M. N. D. S. Cordeiro, S. A. Vázquez, F. J. Aoiz, and L. Bañares

Citation: The Journal of Chemical Physics **119**, 10618 (2003); doi: 10.1063/1.1622387
View online: http://dx.doi.org/10.1063/1.1622387
View Table of Contents: http://scitation.aip.org/content/aip/journal/jcp/119/20?ver=pdfcov
Published by the AIP Publishing

A direct classical trajectory study of the acetone photodissociation on the triplet surface

E. Martínez-Núñez, A. Fernández-Ramos, and M. N. D. S. Cordeiro[a)]
Departamento de Química Física, Facultad de Química, Universidad de Santiago de Compostela, 15782 Santiago de Compostela, Spain

S. A. Vázquez,[b)] F. J. Aoiz, and L. Bañares
Departamento de Química Física, Facultad de Química, Universidad Complutense, 28040 Madrid, Spain

(Received 16 July 2003; accepted 5 September 2003)

Product energy distributions (PEDs) for the photodissociation of acetone at 266, 248, and 193 nm were evaluated by direct classical trajectory calculations on the lowest triplet potential energy surface. CASSCF(8,7) and MRCI+Q calculations were first performed to obtain a set of high-level *ab initio* data with which the semiempirical parameters were refined. The trajectories were initiated at the barrier, using two different microcanonical sampling methods. The results obtained for the excess energies corresponding to excitation at 266 and 248 nm are in good agreement with the experimental product energy partitioning, supporting a dissociation event taking place on the T_1 surface after intersystem crossing from the initially exited S_1 state. At 193 nm, the results obtained with the two sampling methods show significant discrepancies. The PEDs calculated with the anharmonic sampling procedure appear to be consistent with the experimental data. © *2003 American Institute of Physics.* [DOI: 10.1063/1.1622387]

I. INTRODUCTION

Acetone has been the subject of intense experimental studies aimed to unravel the photochemistry of ketones (see Refs. 1–4, and references therein). The photodissociation of these molecules via cleavage of one or the two α-CC bonds, known as Norrish type-I reaction, is the most studied photochemical process in these systems.

The first absorption band in acetone (from 330 to 220 nm, with its maximum around 280 nm) corresponds to an $n\rightarrow\pi^*$ $(S_0\rightarrow S_1)$ transition. This involves promotion of a nonbonding electron on the oxygen to the antibonding π^* orbital. According to fluorescence lifetime measurements,[5–9] the dissociation of acetone upon excitation to the S_1 state is proposed to proceed over an energy barrier on the T_1 surface after an $S_1\rightarrow T_1$ intersystem crossing (ISC). The triplet surface correlates with the electronic ground state of the acetyl and methyl radicals,

$$CH_3COCH_3\rightarrow CH_3CO+CH_3. \quad (1)$$

However, recent femtosecond pump–probe investigations on the photodissociation of acetone have brought out controversies on its dissociation mechanism. Zhong *et al.*[10] and Owrutsky and Baronavski[11] concluded that acetone experiences a prompt dissociation (within 200 fs of excitation) when it is excited at 259 and 260 nm, respectively, indicating direct fragmentation from the initially excited state. Their data were consistent with previous observations reported by Shibata and Suzuki (at 253 nm excitation),[12] but these latter authors made a different interpretation and concluded that the acetone excited state is long-lived (>15 ps). It is worth noting that femtosecond pump–probe experiments may lead to wrong conclusions if fragmentation in the neutral and ionic ladders are not discriminated. In the case of Suzuki's experiment, this discrimination was accomplished from images of photofragment ion distributions. Very recently, Zewail and co-workers (at 307 nm excitation) observed that the S_1 α-cleavage dynamics of acetone is on the nanosecond time scale (with the $S_1\rightarrow T_1$ ISC as the rate-limiting step), in agreement with the previous fluorescence lifetime studies.[5–9] They concluded that the initial motion in the fs time scale observed in their experiments corresponds to the dephasing of the wave packet out of the Franck–Condon region on the S_1 surface.[1]

Measurements of product translational, vibrational, and rotational energies provide relevant information about the potential energy surface on which the dissociation event takes place. A number of such studies appeared in the literature for excitation of acetone to the first absorption band $(S_0\rightarrow S_1)$. Hancock and Wilson[13] used photofragment translational spectroscopy (PTS) to examine the photodissociation dynamics at 266 nm and found that 13.9 kcal/mol on average of the available energy appeared as product translation. At the same excitation energy, Waits *et al.*[14] measured the translational energy of the vibrationless CH_3 radicals by 2+1 resonance enhanced multiphoton ionization (REMPI) with time-of-flight mass spectrometry and obtained a similar value. By PTS, Lee and co-workers[15] studied the photodissociation of acetone following 248 nm excitation. They found that 14.2 ± 1.0 kcal/mol on average of the available energy goes into translation of the photofragments. The large fraction of available energy partitioned into translation led

[a)]Permanent address: Departamento de Química, Faculdade de Ciências, Universidade do Porto, Portugal.
[b)]Permanent address: Departamento de Química Física, Universidad de Santiago de Compostela, Santiago de Compostela, Spain.

them to suggest that the translational energy release is dominated by the exit barrier on the T_1 surface after the $S_1 \rightarrow T_1$ ISC process, ruling out the possibility of direct dissociation on the S_1 surface (which has a very small exit barrier). On the other hand, a substantial fraction ($30 \pm 4\%$) of the nascent acetyl radicals was observed to contain sufficient energy to undergo spontaneous secondary decomposition,

$$CH_3CO \rightarrow CH_3 + CO. \quad (2)$$

Gandini and Hackett found a similar percentage (35%).[16]

The second absorption band ($S_0 \rightarrow S_2$) in acetone results from an $n \rightarrow 3s$ Rydberg excitation. The $S_0 \rightarrow S_2$ band origin lies at 195 nm above S_0. Pilling and co-workers[17] have shown by end analysis that dissociation into two methyl radicals and carbon monoxide accounts for >95% of the photolysis products at 193.3 nm, in agreement with the more recent observations of Owrutski and Baronavski by femtosecond pump–probe experiments.[18] Lee and co-workers[15] in their PTS investigation at 193 nm found that 38% of the available energy corresponds to product translation, and suggested that significant internal energy resides in the nascent CH_3 fragments, in agreement with previous diode laser absorption/gain measurements.[19] They fitted the time-of-flight spectra at 193 nm on the basis of a stepwise mechanism and obtained a primary translational energy distribution peaking at 16 kcal/mol. Also, the results of a barrier impulse model agreed well with the experimental data.[15] Lee and co-workers concluded that the dynamics at 193 nm (which implies an initial $S_0 \rightarrow S_2$ transition) is similar to that at 248 nm ($S_0 \rightarrow S_1$ excitation); that is, it involves an ISC to the T_1 surface on which acetone dissociates. This, however, contrasts with the conclusions inferred by ultrafast mass-resolved photoionization spectroscopy. Specifically, Owrutski and Baronavski (one-photon pumping at 193–195 nm) (Refs. 11 and 18) reported a $3s$ Rydberg state lifetime (which they associated to the primary dissociation) of 4.7 ± 0.2 ps, similar to that of 3.2 ± 0.4 ps reported by Zhong *et al.* (two-photon excitation).[10] The lifetime estimated by Buzza *et al.*[20] using three-photon pumping at 585 nm is much shorter (100 ± 50 fs). Therefore, all these ultrafast studies do not support dissociation from the triplet state, as the ISC is expected to occur on the nanosecond time scale.

Recently, Zewail and co-workers[4] suggested that at 193 nm the primary CC bond cleavage occurs on the S_1 state. A photon of 193 nm may excite acetone to the S_2 state near its 0–0 band, so that the available energy is not sufficient for any reaction to occur from this state.[3,4] The dissociation would take place on the S_1 state, after internal conversion from the S_2 state. To a certain extent, their conclusion is based on the observed kinetic energy releases from dissociation of acetone at 266,[13] 248, and 193 nm.[15] As indicated above, upon excitation to the S_1 state, the average relative translational energy for the primary dissociation was found to be 13.9 kcal/mol (Ref. 13) at 266 nm, and 14.2 kcal/mol (Ref. 15) at 248 nm. For excitation at 193 nm ($S_0 \rightarrow S_2$), Zewail and co-workers considered a value of 7.7 kcal/mol (taken from Ref. 15) as the average (relative) kinetic energy release. Obviously, if for all these wavelengths the dissociation occurred on the same surface, one would expect an increase in the average relative translational energy when a higher excitation energy is used; but this appears not to be the case. However, the value of 7.7 kcal/mol reported by Lee and co-workers[15] does not correspond to the average relative kinetic energy release of the primary dissociation. Rather, the above value refers to the independent fragment translational distribution for the methyl radical in the acetone center-of-mass, which was the approach followed by them due to the inability to resolve the methyl radicals originated from the primary and secondary dissociations. In fact, as indicated above, Lee and co-workers[15] estimated an average relative translational energy of 16 kcal/mol for the primary dissociation, which follows the trend observed for the lower excitation energies (corresponding to 266 and 248 nm). On the other hand, the mechanism proposed by Zewail and co-workers[4] involves a nonadiabatic electronic transition for the acetyl radical ($\tilde{A}\,^2A'' \rightarrow \tilde{X}\,A'$) as the last step previous to the secondary dissociation, but very recently this process was questioned by Zhong *et al.*[21] in an ultrafast photodissociation dynamics study of several ketones at 195 nm.

Theoretical calculations have proved to be very helpful (if not necessary) for unraveling mechanisms in reaction dynamics. In particular, molecular structure calculations on the ground and lowest excited states of acetone[1,22–24] provided a significant contribution to the current picture of the Norrish mechanisms. The CASPT2//CASSCF(8,7)6-31G(d,p) calculations of Liu *et al.*[22] predict that the energies (relative to the S_0 minimum and with ZPE corrections) for the transition states on the T_1 (ts-T_1) and S_1 (ts-S_1) surfaces are 114.2 and 127.8 kcal/mol, respectively. The CASSCF(10,8)/6-31G(d) and time-dependent B3P86/6311++G(d,p)//CASSCF(10,8)/6-31G(d) calculations reported by Zewail and co-workers[1] give relative energies (with ZPE corrections) of 104.7 and 89.5 kcal/mol, respectively, for ts-T_1, and of 118.2 and 112.1, respectively, for ts-S_1. By the second-order multireference Møller–Plesset perturbation method, Sakurai and Kato[24] obtained a relative energy of 87.8 kcal/mol for ts-T_1. This value and the above calculated by time-dependent density functional theory (89.5 kcal/mol) are rather similar to that measured by Zuckermann *et al.*[7] (93.4 kcal/mol). According to these theoretical results, upon excitation to the $3s$ Rydberg state, and assuming a fast internal conversion to the first singlet excited state, the primary dissociation would occur on this S_1 state, with a lifetime on the picosecond scale, as suggested by Zewail and co-workers.[4] However, it is well-known that in general an accurate treatment of excited states may need the use of the more rigorous, highly CPU-time demanding, multireference configuration interaction (MRCI) methods in combination with large basis sets, and so the above theoretical results should be taken with care.

From the theoretical point of view, a further and desirable step to face the controversies and gaps that still remains on the mechanisms of the photodissociation of acetone upon excitation to the S_1 and S_2 states is to carried out dynamics studies. Obviously, a global treatment of the various steps that may comprise the whole mechanism is unfeasible at present. In this study, we report dynamics calculations for the dissociation of acetone on the T_1 surface at 266, 248,

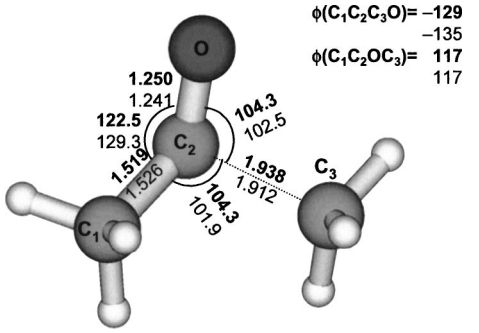

FIG. 1. Transition state (ts1) geometry obtained in this study at the CASSCF/aVDZ level of theory. Selected geometrical parameters at the CASSCF/aVDZ (numbers in boldface) and AM1-SRP levels of theory are indicated in the figure.

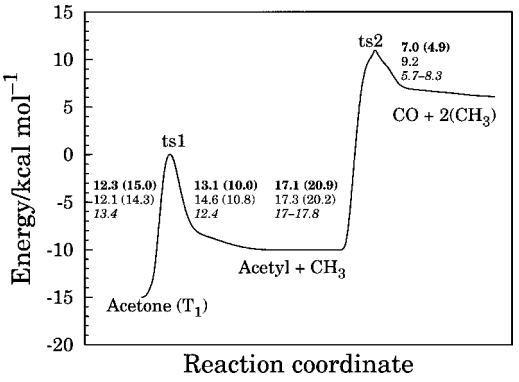

FIG. 2. Minimum energy paths, obtained with our AM1-SRP model PES, involved in the primary and secondary dissociation processes of triplet acetone. Numbers in boldface are AM1-SRP values and numbers in italic are experimental data (Refs. 8, 15, and 35). The *ab initio* data for the secondary dissociation was taken from Ref. 34, and those for the primary dissociation were calculated here at the MRCI+Q level of theory. Values in parentheses refer to energies without the ZPE correction.

and 193 nm. The wavelengths 266 and 248 nm correspond to excitation of acetone to the S_1 surface, and 193 nm to excitation to the S_2 surface. For the last wavelength, the majority of the experimental and theoretical studies suggests that the primary dissociation does not take place on the triplet surface. Even though, we have also selected this wavelength following the suggestion of Lee and co-workers[15] that the dynamics at 193 nm is similar to that at 248 nm (and 266 nm). To the best of our knowledge, this is the first dynamics study on this prototypical system. Specifically, product energy distributions for the primary (CH_3CO and CH_3), and the secondary (CH_3 and CO; only at 193 nm) photoproducts are calculated by direct classical trajectories on a semiempirical potential energy surface (PES) parameterized to fit our own MRCI calculations. The trajectories are started from the transition state on the triplet surface (see Fig. 1) by standard microcanonical sampling procedures. The theoretical results are then compared with the available experimental data.

II. *AB INITIO* CALCULATIONS AND MODEL PES

The *ab initio* calculations were performed at the complete-active-space self-consistent-field (CASSCF) method as well as at the internally contracted multireference configuration interaction (MRCI) with the Davidson cluster correction (Q) approach using the CASSCF configuration space as reference. We used the same active space as Liu *et al.*;[22] specifically, a CAS(8,7) which includes two sets of C–C σ and σ^* orbitals, one set of π and π^* orbitals and a nonbonding orbital of the oxygen atom. In all the calculations the aug-cc-pvdz (aVDZ) basis set was employed.

The geometries of the T_1 reactant and transition state, as well as the product acetyl and CH_3 ground state radicals, with which the T_1 surface correlates, were fully optimized at the CASSCF(8,7)/aVDZ level of theory. The reactant and products were obtained by following the minimum energy path from the transition state in both directions. To characterize the stationary points, a vibrational frequency analysis was also carried out at this level of theory. Dynamical electronic correlation effects were taken into account through single point MRCI+Q calculations at the CASSCF(8,7)/aVDZ optimized stationary points. All the *ab initio* computations were accomplished with the MOLPRO program.[25]

Figure 1 shows the geometry of the transition state in the acetone triplet state surface, and Fig. 2 collects the classical (values in parentheses) and ZPE-corrected energies obtained at the MRCI+Q level (second row of numbers) for the direct and reverse barrier heights of process (1). The barrier height for the primary dissociation (12.1 kcal/mol) is in good agreement with the experimental value (13.4 kcal/mol) and with previous *ab initio* results.[1,22–24] It is important to notice that inclusion of dynamical correlation effects through MRCI+Q calculations reduces the reverse barrier height by 10 kcal/mol. The multireference Møller–Plesset calculations of Sakurai and Kato[24] predict a similar reverse barrier height (13.6 kcal/mol versus 14.6 kcal/mol in our work, with the ZPE corrections).

The model PES for the trajectory calculations consisted in the semiempirical AM1 Hamiltonian supplemented with specific reaction parameters (AM1-SRP),[26] obtained by a fit to the MRCI and CASSCF *ab initio* data of the features of the T_1 surface relevant to the dynamics. These data include some geometrical parameters, the vibrational frequencies of the transition state, and the exit barrier height of the primary dissociation. Figure 2 shows the energy profile for the primary and secondary dissociation processes of acetone on the triplet PES obtained with the AM1-SRP model. The figure includes a comparison with *ab initio* results and experiment. Notice that both the direct barrier height of the primary dissociation and direct and reverse barrier heights of the secondary dissociation are quite well reproduced by the model PES, even though they were not considered in the parameterization process.

Overall, the differences between the *ab initio* (or experimental) data and our PES results are rather small. Figure 1 also shows a comparison between the TS geometry at the CASSCF and AM1-SRP levels of theory. The major difference appears for the $C_1C_2C_3O$ dihedral angle and the C_1C_2O bond angle. The vibrational frequencies and geometries for other stationary points (not shown for simplicity) were also well reproduced by the semiempirical PES.

TABLE I. Product average energies[a] (in kcal/mol) obtained in this study at the three excitation wavelengths.

	266 nm			248 nm			193 nm		
	SM1	SM2	Expt.[b]	SM1	SM2	Expt.[c]	SM1	SM2	Expt.
E_{rans}	14.3	13.8	13.9	16.2	13.8	14.2±1	20.9	15.9	
$E_{yib,acetyl}$	8.0	11.7		11.9	18.0		31.7	38.6	
$E_{rot,acetyl}$	2.6	2.8		2.9	2.5		2.8	2.3	
E_{vib,CH_3}	2.7	−1.3		2.5	0.0		10.4	8.6	
E_{rot,CH_3}	2.0	3.0		2.5	3.3		4.6	5.0	
E_{trans,CH_3}[d]							12.2	10.8	7.7±1;[c] 10.5±1.9[c]
							15.5; 9	11.8; 9.8	
E_{int,CH_3}							7.6	12.9	11.8;[c] 2.6;[e] 8.5[f]
$E_{trans,CO}$							7.5	6.2	4.8±0.5;[c] 8.6[e]
$E_{vib,CO}$							0.1	1.9	2.1[f]
$E_{rot,CO}$							5.9	4.4	

[a]Vibrational energies are given with respect to the corresponding ZPEs (taken from Refs. 34 and 44).
[b]From Ref. 13.
[c]From Ref. 15.
[d]The second row of numbers corresponds to the translational energy of CH_3 for the primary and secondary dissociations, respectively.
[e]From Ref. 38.
[f]From Ref. 39.

III. CLASSICAL TRAJECTORY CALCULATIONS

The trajectories were initiated at the transition state (ts1, see Fig. 1) on the T_1 surface of acetone according to two different sampling methods. The first is a quasiclassical rigid rotor/normal mode model (hereinafter SM1), described in detail elsewhere.[27,28] With this method, a microcanonical ensemble of rovibrational states at the barrier is obtained by assigning n_i, J, K quanta to a given degree of freedom, using the following probability function:

$$P(n_i,J,K)=\frac{N^{ts}_{n_i,J,K}}{N^{ts}_{tot}}, \tag{3}$$

where N^{ts}_{tot} is the total number of rovibrational states at the barrier, and $N^{ts}_{n_i,J,K}$ is the barrier sum of states with a given degree of freedom having a fixed number of quanta. In our study the total angular momentum J was restricted to zero.

The second barrier sampling method employed here (SM2) is based on the efficient microcanonical sampling (EMS) of Nyman, Nordholm, and Schranz,[29,30] which takes into account the full anharmonicity and vibrational coupling of the PES. The most significant change in the present case with respect to the standard EMS procedure is that the Markov walk is performed in normal modes, fixing the reaction coordinate at zero to confine the sampling to the configuration space of the transition state.[31] At each step of the random walk, a transformation to Cartesian coordinates is made to calculate the statistical weight of the configuration, as in the standard procedure.

Each ensemble of trajectories was run at three different energies, corresponding to photon wavelengths of 266, 248, and 193 nm. In each case, the excess energy at ts1 was evaluated as the difference between the excitation energy and the ts1-T_1 energy, relative to the S_0 minimum, determined experimentally (93.4 kcal/mol).[7] Each run consisted of 2000–3000 direct trajectories, which were integrated by using a combined fourth order Runge–Kutta and six-order Adams–Moulton predictor–corrector algorithm with a fixed step size of 0.05 fs, using an extensively adapted version of the GENDYN program,[32] which incorporates the relevant subroutines of MOPAC7.0.[33] During the integration of trajectories, energy conservation of better than five digits was achieved.

For the calculations at 193 nm, the trajectories were halted when 5 ps elapsed or when the distance between the center-of-masses of the acetyl and methyl radicals reached 8 Å and that between the center-of-masses of the methyl radical (of the dissociated acetyl radical) and CO reached 6 Å. For the calculations at 266 and 248 nm, only the first geometrical condition was considered, and the maximum time allowed was 2 ps. Finally, product internal and relative translational energies were computed. Product translational distributions were fitted by the method of Legendre moments to continuous curves.

IV. RESULTS AND DISCUSSION

A. Dissociation at 266 and 248 nm

Table I shows a comparison between our theoretical product average energies and some experimental results. At 266 nm, the trajectory results obtained with both SM1 and SM2 predict that the average relative translational energy for the primary dissociation is around 14 kcal/mol, in agreement with the experimental value of 13.9 kcal/mol. The average vibrationally energy content of the acetyl radical, 8.0 and 11.7 kcal/mol (above the ZPE, taken from Ref. 34), respectively, is well below the secondary dissociation barrier (17±1 kcal/mol).[35] The percentage of acetyl radicals formed with internal energy above this barrier (i.e., the percentage of acetyl radicals that would undergo a secondary decomposition) is about 2%–4% (for SM1) and 22%–30% (for SM2) (the range of values comes from the experimental uncertainty in the barrier height of the acetyl radical). Gandini and Hackett[16] found that 16%–19% of the acetone molecules that

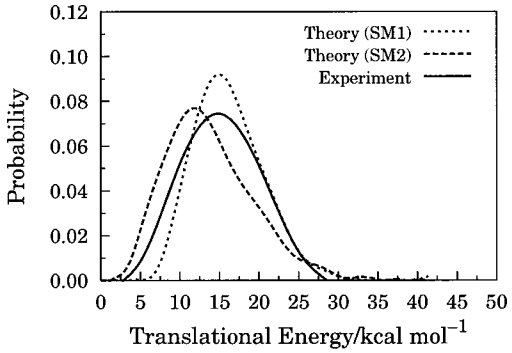

FIG. 3. Relative translational energy distributions obtained for the primary dissociation at 248 nm. The experimental distribution was taken from Ref. 15.

photolyze at 265 nm undergo a secondary dissociation giving rise to $2CH_3+CO$, which is within the range of predicted values.

For excitation at 248 nm, the average relative translational energies obtained in our study, 13.8 kcal/mol and 16.2 kcal/mol for SM2 and SM1, respectively, are in good accord with the experimental value of 14.2 kcal/mol. In more detail, the translational energy distribution computed at 248 nm is compared in Fig. 3 with that determined experimentally by Lee and co-workers.[15] As can be seen, the agreement between theory and experiment is reasonably good, which supports the earlier conclusions that the dissociation process takes place on the triplet surface.[4–9,15] Note that, although the excitation energy changes from 266 to 248 nm (i.e., it increases by ~8 kcal/mol), our results for SM2 predict the same average translational energy, while for SM1 the translational energy rises by 2 kcal/mol. We will discuss in a separate section the differences between these two sampling methods and their implications on the computed product energy distributions.

The average vibrational energy content of the acetyl radical calculated at 248 nm is about 4 kcal/mol (SM1) or 6 kcal/mol (SM2) higher than that obtained at 266 nm. At the former wavelength, the percentage of trajectories that may experience secondary dissociation is about 15%–25% for SM1 and 50%–60% for SM2. The experimental values of 30% and 35%, as determined by North *et al.*[15] and Gandini *et al.*,[16] respectively, are again within the range formed by the SM1 and SM2 results.

Finally, it should also be noted that the acetyl radicals produced in the photodissociations at 248 nm and 266 nm are rotationally excited with 2.5–2.9 kcal/mol. The results for both the SM1 and SM2 methods predict a strong preference for rotational excitation around the *a*-axis rather than around axes *b* and *c*. Since the acetyl radical presents rotational metastability around the *a*-axis (which is roughly along the C–C axis), the rotational energy around this axis would be unavailable to couple with the reaction coordinate (see Refs. 36 and 37 for a discussion on this issue and the influence of rotational metastability on the lifetimes of the acetyl radical).

B. Dissociation at 193 nm

The (independent fragment) CH_3 and CO translational energy distributions predicted in this study for excitation at 193 nm are compared in Fig. 4 with those determined experimentally by Lee and co-workers.[15] From the plots it is clear that the results obtained under SM2 are in reasonable agreement with the experimental data. In general, the theoretical distributions are shifted towards higher translational energies in comparison with the experimental ones, which contrasts with the results at 248 nm. This might indicate that a different surface (presumably S_1) is involved in the dynamics. This shift is reflected by the CH_3 and CO average translational energies. Thus, for the case of SM2 initialization, the theoretical results are 10.8 and 6.2 kcal/mol, respectively (see Table I), which are somewhat higher than the experimental values of 7.7 ± 1 kcal/mol and 4.8 ± 0.5 kcal/mol, respectively.[15] It is important to note that it was experimentally unfeasible to distinguish between the methyl radicals originated from the primary and secondary dissociations. This is consistent with our SM2 prediction that the primary and secondary average CH_3 translational energies are rather similar; specifically, 11.8 and 9.8 kcal/mol, respectively. Trentelman *et al.*[38] reported a value of 10.5 ± 1.9 kcal/mol for the CH_3 average translational energy at 193 nm, which is higher than that obtained by North *et al.*[15] However, as the latter authors[15] pointed out, the CH_3 0_0^0 Q branch, probed in that experiment,[38] reflects the kinetic energy of only the vibrationless methyl radicals. If a large fraction of the available energy resides in the CH_3 fragments as Hall *et al.*[19] and North *et al.*[15] suggested, then the translational energy reported by Trentelman *et al.*[38] is not representative of the overall dissociation dynamics. The values of Hall *et al.* (8.5 kcal/mol) and North *et al.* (11.8 kcal/mol) for the CH_3 internal energy are in between the trajectory results obtained by SM1 and SM2 (7.6 and 12.9 kcal/mol, respectively). The value reported by Trentelman *et al.* (2.6 kcal/mol) (Ref. 38) is clearly underestimated.

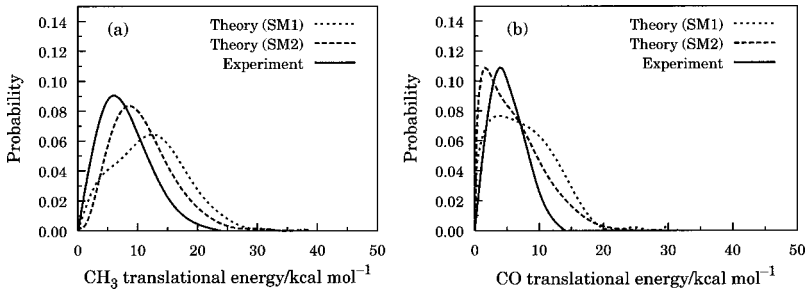

FIG. 4. (a) CH_3 and (b) CO translational energy distributions relative to the acetone center of mass, obtained at 193 nm excitation. The experimental distributions were taken from Ref. 15.

TABLE II. CO vibrational populations obtained in the 193 nm photodissociation of acetone.

	SM1 (this work)	SM2 (this work)	Expt.[a]	Expt.[b]
$v=0$	0.86±0.03	0.71 ±0.02	0.73	0.73
$v=1$	0.12±0.03	0.21 ±0.02	0.20	0.21
$v=2$	0.01±0.01	0.058±0.011	0.07	0.045
$v=3$	0.003±0.004	0.017±0.006	≤0.03	0.008
$v=4$	0	0.004±0.003		0.003

[a]From Ref. 38.
[b]From Ref. 19; the vibrational distribution was obtained by measurements for $v \geq 1$ and surprisal extrapolation for $v=0$.

The vibrational energy content of the CO product determined by Hall *et al.*[39] (2.1 kcal/mol) is in excellent agreement with our value of 1.9 kcal/mol calculated under SM2. Furthermore, as shown in Table II, the CO vibrational populations obtained in the present study with SM2 are in very good accordance with the experimental results.[38,39] In order to complete the analysis of the product energy distributions, we show in Fig. 5 a comparison between the theoretical and experimental CO product rotational distributions. As can be seen, the agreement between the SM2 results and the distributions of Trentelman *et al.*[38] is quite good.

Pilling and co-workers[17] have shown by end analysis that the dissociation into two methyl radicals and carbon monoxide accounts for >95% of the photolysis products at this wavelength. The results obtained here for the acetyl radical internal energy lead to 93%–96% and 97%–99% of secondary dissociations as predicted by SM1 and SM2, respectively, in good agreement with the experimental determination. A primary issue in the photodissociation of acetone was whether the primary and secondary dissociations were concerted or stepwise, especially at the high excitation energies. Through combination of product studies and ultrafast spectroscopy, it has been demonstrated that for all the electronically excited states investigated to date, dissociation takes place in a stepwise manner. Our calculations show that most of the trajectories are stepwise, in agreement with experiment. The average number of oscillations in the acetyl C–C(O) bond before its cleavage was 3 for SM2 and 33 for SM1. Considering a C–C(O) stretching frequency of about 1100 cm^{-1}, we estimated acetyl lifetimes of ~0.1 ps (SM2) or 1.0 ps (SM1). The acetyl lifetime estimated for SM1 is of the same order to those determined in the femtosecond experiments of Zhong *et al.* (1.7 ps),[10] Buzza *et al.* (1.75 ps),[20] and Owrutski and Baronavski (3.1±0.5 ps),[11,18] wherein acetone was initially excited to the 3*s* Rydberg state. The lifetime estimated with SM2 is one order of magnitude smaller.

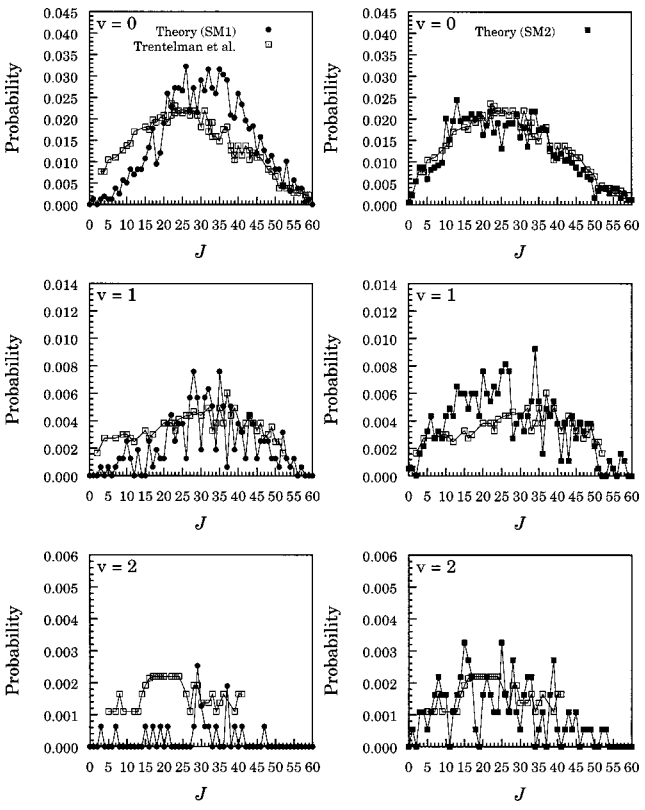

FIG. 5. Rotational distributions (for $v=0-2$) of the CO product obtained for the 193 nm photodissociation of acetone. The experimental distributions were taken from Ref. 38.

In general, the results obtained in the present work under SM2 at 193 nm appear to be consistent with a mechanism in which the dissociation occurs on the triplet state as stated by Lee and co-workers.[15] However, dissociation on the S_1 state, as proposed by Zewail and co-workers[4] (and detailed in the Introduction), should not be ruled out without further investigation. In principle, the very small exit barrier obtained by CASSCF calculations for the S_1 surface (<1.0 kcal/mol) (Ref. 1) does not seem to be consistent with the observed translational energy distributions. However, Zewail and co-workers[1] predicted an S_1/S_0 conical intersection (CI), having a dissociating C–C bond of about 2.9 Å and an almost linear CCO bond angle (169.7°) in the acetyl fragment, which may be involved in the dynamics if the dissociation occurred in the S_1 state. If so, funneling through this CI could have important consequences; in particular, it might increase the translational energy of the primary dissociation in comparison with a fragmentation occurring entirely on the S_1 surface.

C. Comparison between SM1 and SM2 sampling methods

It is interesting to make a comment on the differences between samplings SM1 and SM2, even though this has been fully discussed elsewhere.[31,40] Model SM1 involves a harmonic and separable Hamiltonian, whereas SM2 takes into account the full anharmonicity and vibrational couplings of the model PES. In the present study these differences have a significant influence on the results at 193 nm, since after the primary dissociation process the acetyl radical has enough energy to decompose. Figure 6 shows a comparison between the configuration spaces spanned by the two sampling methods. Specifically, plots (a)–(c) show the projection onto the OC_2C_3 plane of the sampled points at the three excitation energies with SM1, and plots (d)–(f) show the corresponding points for SM2. The most important differences concern the configuration space sampled by C_1 (the one that belongs to the acetyl radical after the primary dissociation). As seen in

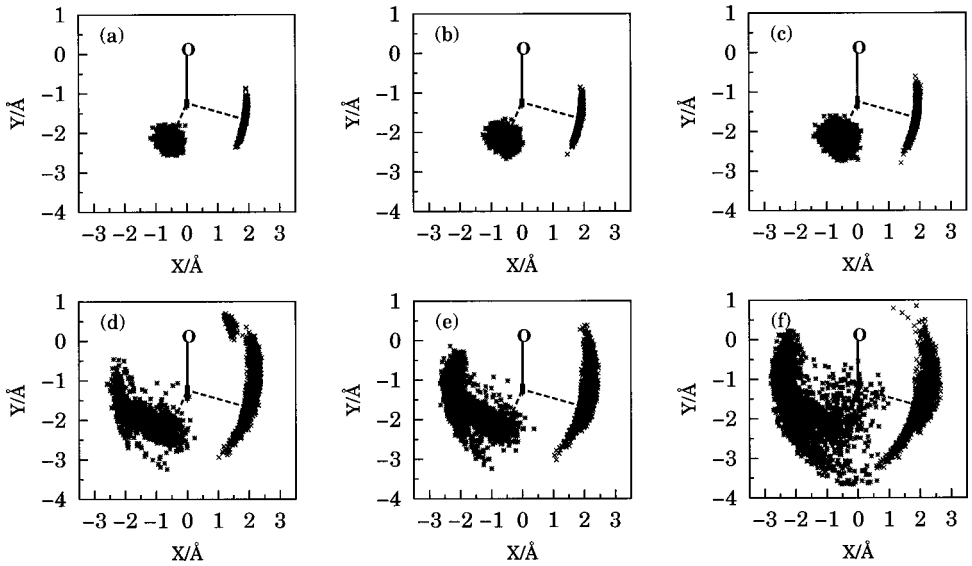

FIG. 6. Projection onto the OC_2C_3 plane at ts1 of the points sampled by (a) SM1 at 266 nm, (b) SM1 at 248 nm, (c) SM1 at 193 nm, (d) SM2 at 266 nm, (e) SM2 at 248 nm, and (f) SM2 at 193 nm.

the figure, due to the harmonic nature of SM1 this carbon atom is confined in a very narrow region of the configuration space. By contrast, because the normal modes associated with the movement of C_1 and C_2 are quite anharmonic, SM2 sweeps a wider region of the configuration space, leading to a higher vibrational energy content of the acetyl radical, as our results indicate. According to our previous comparison between the experimental and theoretical percentages of acetyl radicals that experience a secondary dissociation, it appears that SM1 underestimates the vibrational energy content in the acetyl radical, whereas SM2 overestimates it. On the other hand, we found the reverse trend for the computed average vibrational energy of the methyl radical produced in the primary dissociation. For excitation at 266 nm the value predicted under SM2 initialization (−1.3 kcal/mol) show some leakage of ZPE. While it has been shown that for certain systems both sampling schemes produce similar results,[41–43] in the photodissociation of acetone, and particularly at the wavelength of 193 nm, the discrepancies appear to be more important. Although the SM2 calculations most closely mimic the experimental results, we have also presented the results obtained with the quasiclassical rigid rotor/normal mode model because this sampling is widely used in trajectory calculations.

V. CONCLUSIONS

In this work, product energy distributions for the photodissociation of acetone at 266, 248, and 193 nm were computed assuming that the dissociation event takes place on the T_1 surface. The calculations involved direct classical trajectories using a semiempirical Hamiltonian with specific parameters fitted to reproduce selected high level *ab initio* data. The trajectories were initialized at the transition state, using two microcanonical sampling models.

For all the selected energies, the theoretical product energy distributions, especially those obtained with SM2, are found to be in reasonably good agreement with the available experimental data. Our results, therefore, are consistent with the previous studies in which it was concluded that the dissociation occurs on the T_1 surface.[4–9,15] However, and in particular for excitation at 193 nm, the mechanism proposed recently by Zewail and co-workers[4] in which the dissociation event would take place on the S_1 surface should not be disregarded without further investigations.

ACKNOWLEDGMENTS

E.M.-N. and A.F.-R. thank the Spanish Ministry of Science and Technology for their Ramón y Cajal research contracts. M.N.D.S.C. thanks Fundação para a Ciência e Tecnologia (Lisbon) for a sabbatical grant (SHFR/BSAB/274/2002). Financial support from the Spanish Ministry of Science and Technology (Grants Nos. BQU2000-0462 and BQU2002-04627-C02-02) and from the European Commission within the RT Network (Contract No. HPRN-CT-1999-00007) is gratefully acknowledged.

[1] E. W.-G. Diau, C. Kötting, and A. H. Zewail, Phys. Chem. Chem. Phys. **2**, 273 (2001).
[2] E. W.-G. Diau, C. Kötting, and A. H. Zewail, Phys. Chem. Chem. Phys. **2**, 294 (2001).
[3] E. W.-G. Diau, C. Kötting, T. I. Sølling, and A. H. Zewail, Phys. Chem. Chem. Phys. **3**, 57 (2002).
[4] T. I. Sølling, E. W.-G. Diau, C. Kötting, S. De Feyter, and A. H. Zewail, Phys. Chem. Chem. Phys. **3**, 79 (2002).
[5] G. M. Breuer and E. K. C. Lee, J. Phys. Chem. **75**, 989 (1971).
[6] O. Anner, H. Zuckermann, and Y. Haas, J. Phys. Chem. **89**, 1336 (1985).
[7] H. Zuckermann, B. Schmits, and Y. Haas, J. Phys. Chem. **92**, 4835 (1988).
[8] H. Zuckermann, B. Schmits, and Y. Haas, Chem. Phys. Lett. **151**, 323 (1988).
[9] H. Zuckermann, B. Schmits, and Y. Haas, J. Phys. Chem. **93**, 4083 (1989).
[10] Q. Zhong, L. Poth, and A. W. Castleman, Jr., J. Chem. Phys. **110**, 192 (1999).
[11] J. C. Owrutsky and A. P. Baronavski, J. Chem. Phys. **110**, 11206 (1999).
[12] T. Shibata and T. Suzuki, Chem. Phys. Lett. **262**, 115 (1996).
[13] G. Hancock and K. R. Wilson, in Proceedings of the IVth International Symposium on Molecular Beams Cannes, France, 1973.

[14] L. D. Waits, R. J. Horwitz, and J. A. Guest, Chem. Phys. **155**, 149 (1991).
[15] S. W. North, D. A. Blank, J. D. Gezelter, C. A. Longfellow, and Y. T. Lee, J. Chem. Phys. **102**, 4447 (1995).
[16] A. Gandini and P. A. Hackett, J. Am. Chem. Soc. **99**, 6195 (1977).
[17] P. D. Lightfoot, S. P. Kirwan, and M. J. Pilling, J. Phys. Chem. **92**, 4938 (1988).
[18] J. C. Owrutsky and A. P. Baronavski, J. Chem. Phys. **108**, 6652 (1998).
[19] G. E. Hall, D. Vanden Bout, and T. Sears, J. Chem. Phys. **94**, 4182 (1991).
[20] S. A. Buzza, E. M. Snyder, and A. W. Castleman, Jr., J. Chem. Phys. **104**, 5040 (1996).
[21] Q. Zhong, D. A. Steinhurst, A. P. Baronavski, and J. C. Owrutsky, Chem. Phys. Lett. **370**, 609 (2003).
[22] D. Liu, W. Fang, and X. Fu, Chem. Phys. Lett. **325**, 86 (2000).
[23] O. Setokuchi, S. Matuzawa, and Y. Shimizu, Chem. Phys. Lett. **284**, 19 (1998).
[24] H. Sakurai and S. Kato, J. Mol. Struct.: THEOCHEM **461**, 145 (1999).
[25] MOLPRO is a package of *ab initio* programs written by H.-J. Werner and P. J. Knowles, with contributions from R. D. Amos, A. Bernhardsson, A. Berning *et al.*
[26] A. González-Lafont, T. Truong, and D. G. Truhlar, J. Phys. Chem. **95**, 4618 (1991).
[27] C. Doubleday, K. Bolton, G. H. Peslherbe, and W. L. Hase, J. Am. Chem. Soc. **118**, 9922 (1996).
[28] K. Bolton, W. L. Hase, and G. H. Peslherbe, *Modern Methods for Multidimensional Dynamics in Chemistry* (World Scientific, Singapore, 1998).
[29] G. Nyman, S. Nordholm, and H. W. Schranz, J. Chem. Phys. **93**, 6767 (1990).
[30] H. W. Schranz, S. Nordholm, and G. Nyman, J. Chem. Phys. **94**, 1487 (1991).
[31] E. Martínez-Núñez, S. A. Vázquez, and A. J. C. Varandas, Phys. Chem. Chem. Phys. **4**, 279 (2002).
[32] D. L. Thompson, GENDYN program.
[33] J. P. P. Stewart, MOPAC7.0, a General Molecular Orbital Package QCPE, 1993, p. 455; J. P. P. Stewart, J. Comput. Chem. **10**, 209 (1989).
[34] S. Deshmukh, J. D. Myers, S. S. Xantheas, and W. P. Hess, J. Phys. Chem. **98**, 12535 (1994).
[35] S. W. North, D. A. Blank, and Y. T. Lee, Chem. Phys. Lett. **222**, 38 (1994).
[36] T. Shibata, H. Li, H. Katayanagi, and T. Suzuki, J. Phys. Chem. A **102**, 3643 (1998).
[37] E. Martínez-Núñez and S. A. Vázquez, Chem. Phys. Lett. **316**, 471 (2000).
[38] K. A. Trentelman, S. H. Kable, D. B. Moss, and P. L. Houston, J. Chem. Phys. **91**, 7498 (1989).
[39] G. E. Hall, H. W. Metzler, J. T. Muckerman, J. M. Preses, and R. E. Weston, Jr., J. Chem. Phys. **102**, 6660 (1995).
[40] E. Martínez-Núñez and S. A. Vázquez, J. Phys. Chem. A **105**, 4808 (2001).
[41] E. Martínez-Núñez, C. M. Estévez, J. R. Flores, and S. A. Vázquez, Chem. Phys. Lett. **348**, 81 (2001).
[42] E. Martínez-Núñez, A. Fernández-Ramos, A. Peña-Gallego, and S. A. Vázquez, Chem. Phys. Lett. **369**, 1 (2003).
[43] E. Martínez-Núñez, A. Fernández-Ramos, S. A. Vázquez, F. J. Aoiz, and L. Bañares, J. Phys. Chem. A **107** 7611 (2003).
[44] Data from NIST Standard Reference Database 69-July 2001 Release: NIST Chemistry WebBook.